Tiny, yet impactful

Journal of Colloid and Interface Science 652 (2023) 1994–2004

Contents lists available at ScienceDirect

Journal of Colloid And Interface Science

journal homepage: www.elsevier.com/locate/jcis

Tiny, yet impactful: Detection and oxidative stability of very small oil droplets in surfactant-stabilized emulsions

Sten ten Klooster [a,1], Machi Takeuchi [b,c,1], Karin Schroën [a], Remco Tuinier [b,c], Rick Joosten [b,d], Heiner Friedrich [b,c,d,*], Claire Berton-Carabin [a,e,*]

[a] Laboratory of Food Process engineering, Wageningen University, P.O. Box 17, Bornse Weilanden 9, 6708 WG Wageningen, the Netherlands
[b] Laboratory of Physical Chemistry, Department of Chemical Engineering and Chemistry, Eindhoven University of Technology, P.O. Box 513, 5600 MB, Eindhoven, the Netherlands
[c] Institute for Complex Molecular Systems, Eindhoven University of Technology, P.O. Box 513, 5600 MB Eindhoven, the Netherlands
[d] Center for Multiscale Electron Microscopy, Department of Chemical Engineering and Chemistry, Eindhoven University of Technology, P.O. Box 513, 5600 MB Eindhoven, the Netherlands
[e] INRAE, BIA, 44000 Nantes, France

GRAPHICAL ABSTRACT

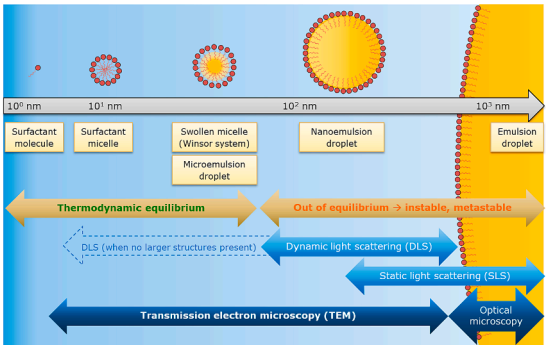

ARTICLE INFO

Keywords:
Emulsion
Droplets
Swollen micelles
Surfactants
Nanoemulsion
Cryo-transmission electron microscopy (TEM)
Dynamic light scattering
Lipid oxidation

ABSTRACT

Hypothesis: The shelf life of multiphase systems, e.g. oil-in-water (O/W) emulsions, is severely limited by physical and/or chemical instabilities, which degrade their texture, macroscopic appearance, sensory and (for edible systems) nutritional quality. One prominent chemical instability is lipid oxidation, which is notoriously complex. The complexity arises from the involvement of many physical structures present at several scales (1–10,000 nm), of which the smallest ones are often overlooked during characterization.

Experiments: We used cryogenic transmission electron microscopy (cryo-TEM) to characterize the coexisting colloidal structures at the nanoscale (10–200 nm) in rapeseed oil-based model emulsions stabilized by different concentrations of a nonionic surfactant. We assessed whether the oxidative and physical instabilities of the smallest colloidal structures in such emulsions may be different from those of larger colloidal structures.

* Corresponding authors.
E-mail addresses: Sten.tenklooster@wur.nl (S. ten Klooster), m.takeuchi@tue.nl (M. Takeuchi), Karin.schroen@wur.nl (K. Schroën), r.tuinier@tue.nl (R. Tuinier), r.r.m.joosten@tue.nl (R. Joosten), H.Friedrich@tue.nl (H. Friedrich), claire.berton-carabin@inrae.fr (C. Berton-Carabin).
[1] Both authors contributed equally to the work.

https://doi.org/10.1016/j.jcis.2023.09.005
Received 31 December 2022; Received in revised form 1 September 2023; Accepted 1 September 2023
Available online 4 September 2023

Winsor system
Microemulsion

Findings: By deploying cryo-TEM, we analyzed the size of very small oil droplets and of surfactant micelles, which are typically overlooked by dynamic light scattering when larger structures are concomitantly present. Their size and oil content were shown to be stable over incubation, but lipid oxidation products were overrepresented in these very small droplets. These insights highlight the importance of the fraction of "tiny droplets" for the oxidative stability of O/W emulsions.

1. Introduction

Oil-in-water (O/W) emulsions can be found in a plethora of industrial products such as foods, paints, pharma and cosmetics [1,2]. These emulsions typically consist of three distinct regions: the core of the oil droplets, the oil–water interface and the continuous phase, of which the latter often contains a substantial amount of non-adsorbed emulsifiers [3,4]. Emulsions have a limited shelf life because of physical and/or chemical instabilities [3]. A prominent phenomenon of chemical instability is lipid oxidation, which is a reaction between oxygen and a labile lipid substrate such as polyunsaturated fatty acids (PUFAs) [5]. Lipid oxidation leads to: a rancid flavor/odor; possible changes in appearance (e.g., discoloring); or the loss of nutrients and bioactive ingredients [3,5,6]. The main physical instabilities are: gravitational separation (creaming, sedimentation); coalescence; Ostwald ripening; or flocculation [7,8]. Physical instabilities often lead to a change in texture and/or appearance. These oxidative and physical instabilities are complex and therefore difficult to control because the aforementioned phenomena occur at various time- and length scales [9]. Moreover, the physical structure of emulsions affects the oxidative stability and vice versa [4,9].

Emulsions often consist of multiple colloidal structures covering a broad range of sizes, from a few nanometers to tens of micrometers [9]. For instance, it is known that small (100–200 nm), and even very small droplets (<100 nm), can be co-existing with larger ones [10]. Commonly, three typical systems differing in droplet size are distinguished (Fig. 1): (i) microemulsions, (ii) nanoemulsions, and (iii) emulsions. We provide a definition for these typical systems in the next lines. (i) In microemulsions or Winsor systems, surfactant micelles (possibly including co-surfactants) contain small amounts of lipids in their hydrophobic core. The curvature of these so-called swollen micelles corresponds to a favorable arrangement of the surfactant molecules, which thereby minimizes the free energy of the system [11]. Moreover, the large magnitude of the (configurational) entropy also contributes to the minimization of the free energy [12]. This results in isotropic and thermodynamically stable systems with droplets of typically 10–50 nm in diameter [13]. (ii) Nanoemulsions, generally defined as emulsions having droplet sizes below 100 nm, are thermodynamically unstable (i.e., at most, metastable), which makes them different from microemulsions. A large external energy supply is required for their formation [13]. (iii) Emulsions, which have droplet sizes above 100 nm, are thermodynamically unstable, and also require an energy input through an *ad hoc* homogenization procedure. The latter two can be stabilized *kinetically*. In this paper, we will assess the presence of the structures termed above and intentionally avoid referring to microemulsions, as the term is generally associated to spontaneous emulsification. This is why we will speak about micelles, very small droplets (i.e., swollen micelles and droplets <100–200 nm) and large droplets, which can all coexist in emulsions encountered in practical systems, such as food matrices [10].

The effect of the physical structure of emulsions on their oxidative stability has received great interest in literature, but is yet far from being understood [3,4,14,15]. For example, small colloidal structures have been postulated to play a decisive role in the lipid oxidation pathways by transferring reactive molecules from one droplet to another [16–19],

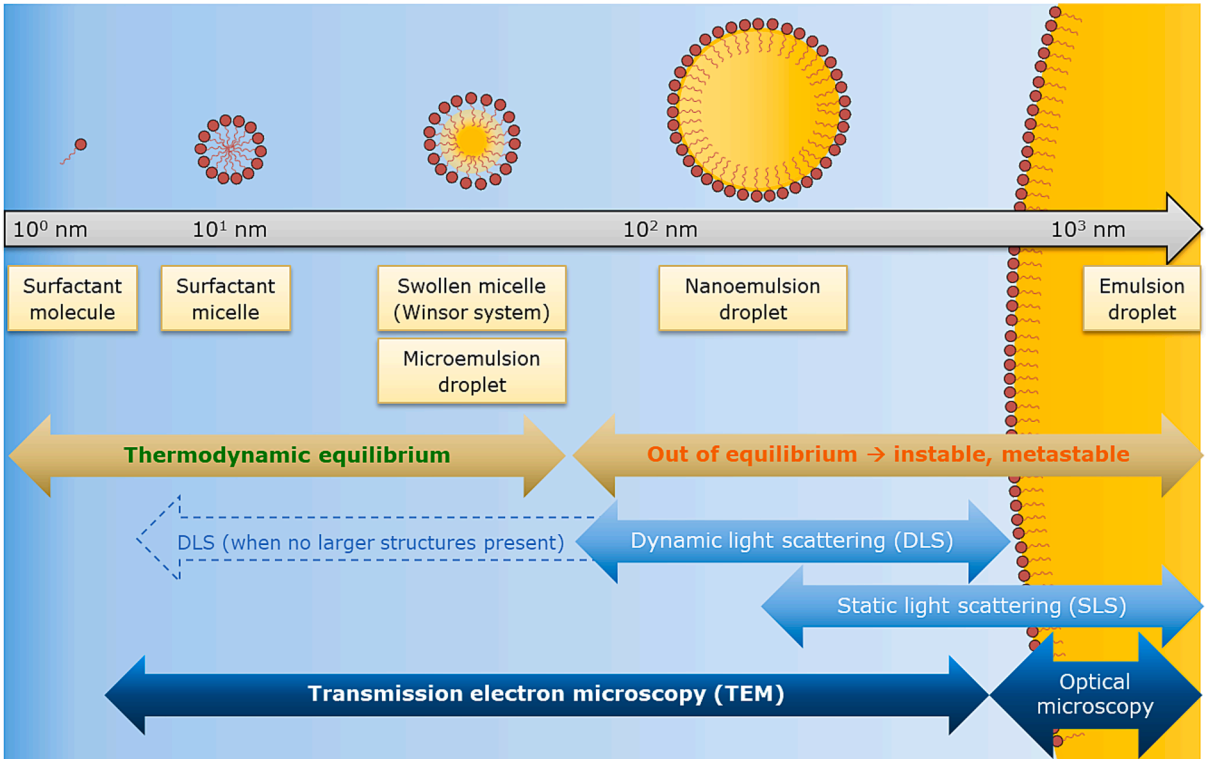

Fig. 1. Schematics of structures that can be present in surfactant-stabilized emulsions, differing in sizes, that can be distinguished by their terminology and the equipment with which they can be detected.

although a recent study from our group has shown that this only occurs for low molar mass and relatively hydrophilic lipid oxidation products [20]. Another example relates to the effect of droplet size on lipid oxidation. It has been suggested that small droplets oxidize faster than large ones due to their larger specific surface area, where lipids can react with pro-oxidants present in the continuous phase, such as metal ions. These metal-catalyzed initiation reactions result in radical formation (Reactions 1–3) [21], even when only trace amounts of metal ions are present [14,22–24]. Initiation reactions can also occur without catalysts, which is especially expected at higher temperatures (Reaction 4). In turn, the favored initiation will result in higher concentrations of radicals, which will cause rapid propagation of lipid oxidation (Reactions 5 & 6) [4]. In practice, contradicting conclusions have been reported on the effect of droplet size on lipid oxidation [4]. Some results in literature indeed show that small droplets oxidize faster [25–35], whereas others indicate that larger droplets oxidize faster [32,34–41], or that droplet size does not influence lipid oxidation [24,30,31,33,34,40,42–44]. There are even studies that found a faster oxidation of small droplets when using soybean oil, whereas the opposite effect was found when using fish oil [32]. The exact cause of these seemingly contradicting findings is not yet known. To the best of our knowledge, there are only two studies in which the effect of droplet size on lipid oxidation was studied in one single polydisperse emulsion [25,33], which is advantageous because the continuous phase has the same composition for both size classes. In both studies, lipid oxidation was shown to proceed faster in the small droplets, although the differences were small, and for certain systems no difference was found [33].

$$LOOH + Fe^{3+} \rightarrow LOO^{\cdot} + H^{+} + Fe^{2+} \text{(Reaction 1)}$$

$$LOOH + Fe^{2+} \rightarrow LO^{\cdot} + OH^{-} + Fe^{3+} \text{(Reaction 2)}$$

$$LH + Fe^{3+} \rightarrow L^{\cdot} + H^{+} + Fe^{2+} \text{(Reaction 3)}$$

$$LH \rightarrow L^{\cdot} + H^{+} \text{(Reaction 4)}$$

$$LO^{\cdot}/LOO^{\cdot} + LH \rightarrow LOH/LOOH + L^{\cdot} \text{(Reaction 5)}$$

$$L^{\cdot} + O_2 \rightarrow LOO^{\cdot} \text{(Reaction 6)}$$

An important first step to get to an improved understanding of the interrelated physical and oxidative instabilities at play is to characterize the colloidal structures present over the relevant size span. To date, such characterization is generally conducted by static light scattering (SLS) or dynamic light scattering (DLS). Light scattered by an emulsion scales with the droplet volume squared. Therefore, these techniques are not equipped well to detect very small structures (<100–200 nm) when they coexist with larger droplets, since the latter largely diminish the contribution of small ones to the measured signal, which scales with the diameter to the power of 6 [10,45]. The deployment of other characterization techniques, such as electron microscopy, is therefore needed. Among electron microscopy techniques, cryogenic transmission electron microscopy (cryo-TEM) can be used to gain insights into sub-micrometer structures in liquid emulsions with nanometer resolution, as samples can be cryogenically fixed and preserved using plunge vitrification [46].

In the present study, we characterized the fraction of very small droplets (typically <200 nm) in rapeseed oil-based model emulsions stabilized by a nonionic surfactant with a versatile range of characterization techniques: dynamic light scattering (DLS), cryogenic transmission electron microscopy (cryo-TEM), and oil content determination in the relevant fractions. We explored the oxidative and physical stability of this fraction of very small droplets co-present in emulsions and of the emulsions as a whole.

2. Materials and methods

2.1. Materials

Rapeseed oil was kindly provided by Unilever (Wageningen, Netherlands) and stripped with alumina powder (MP EcoChromet ALUMINA N, Activity: Super I, Biomedicals) to remove impurities and endogenous antioxidants, in particular tocopherols [47]. Deuterated chloroform and dimethylsulfoxide ($CDCl_3$ and DMSO-d_6) were purchased from Euriso-top (Saint-Aubin, France). *n*-Hexane and 2-propanol were obtained from Actu-All Chemicals (Oss, the Netherlands). Polysorbate 20 (Tween 20) and ethylenediamine tetraacetic acid calcium disodium salt (EDTA) were purchased from Sigma (Sigma-Aldrich, Zwijndrecht, the Netherlands). Ultrapure water (18.2 MΩ) was used for all experiments and prepared using a Milli-Q system (Millipore Corporation, Billerica, MA, USA). Assay reagent and standard for triacylglycerols (Triglycerides liquicolor mono kit) for a colorimetric quantification method were purchased from HUMAN (HUMAN Gesellschaft für Biochemica und Diagnostica mbH, Wiesbaden, Germany). The assay reagent content was: 50 mmol/L PIPES buffer (pH 7.5), 5 mmol/L 4-chlorophenol, 0.25 mmol/L 4-aminoantipyrine, 4.5 mmol/L magnesium ions, 2 mmol/L ATP, 1.3 U/mL lipases, 0.5 U/mL peroxidase, 0.4 U/mL glycerol kinase and 1.5 U/mL glycerol-3-phosphate oxidase.

2.2. Emulsion preparation

Either 0.5 or 2.0 wt% of Tween 20 were added to 10 mM sodium phosphate buffer (pH = 7.0) and stirred for 30 min. For the samples that were used for cryo-TEM analysis and DLS, ultrapure water was used instead of phosphate buffer because the buffer resulted in lower contrast between Tween micelles and the background, and hence impeded interpretation of cryo-TEM images. Stripped rapeseed oil (10 wt%) was added to the continuous phase to form a coarse emulsion by high-speed stirring at 11,000 rpm for 1 min with a rotor–stator homogenizer (Ultra-turrax IKA T18 basic, Germany). To produce a somewhat finer emulsion, this coarse emulsion was passed two times through a lab scale colloid mill with gap width of 0.32 mm (IKA Magic Lab, Staufen, Germany), operated for 2 min at 26,000 rpm, and cooled with water at 4 °C. To produce an emulsion with even smaller average droplet size, the coarse emulsion was passed three times through a high-pressure homogenizer (M−110Y Microfluidizer, Microfluidics, Massachusetts, USA) equipped with a F12Y interaction chamber, which was operated at 600 bars and cooled with ice. For one of the colloid mill-made emulsions, EDTA (75 mg/kg continuous phase) was added after emulsification. These emulsions were either incubated, as described below (colloid mill-made emulsions), or used directly for further measurements (all emulsions).

2.3. Incubation and sample taking

The 0.5- wt% Tween 20-based emulsion in buffer made with the colloid mill was incubated as follows: ten milliliters of emulsion were placed into 20-mL headspace vials and incubated at 25 °C while rotating horizontally at 2 rpm in the dark. At selected time points, the content of two headspace vials was pooled into a 50-mL centrifuge tube. Next, 1.5 mL was taken for measurements on the whole emulsion, whereas the rest of the emulsion was centrifuged at 28,000 × *g* and 20 °C for 30 min (in duplicate). The phase containing very small droplets (<200 nm) remained as a subnatant phase below a creamed layer. This subnatant was collected by making a hole at the bottom of the tube. 1.5 mL were taken that were used directly for the physical characterization measurements. For the extractions and lipid oxidation measurements, the samples were first stored under inert gas at −80 °C for 48 h to 20 days.

2.4. Measurements

2.4.1. Size measurements

2.4.1.1. Static light scattering. The oil droplet size (diameter) and size distribution in the emulsions was assessed by static light scattering (SLS) (Malvern Mastersizer 3000, Malvern Instruments Ltd., Malvern, Worcestershire, UK), using a refractive index of 1.47 for the dispersed phase and 1.33 for the dispersant (water); and an absorption index of 0.01.

2.4.1.2. Dynamic light scattering. The size of the colloidal structures present in the emulsions' subnatant phase (section 2.3) was assessed by dynamic light scattering (DLS) (Zetasizer Nano ZS, Malvern Instruments Ltd., Malvern, Worcestershire, UK), using a refractive index of 1.47 for the dispersed phase and 1.33 for the dispersant (water) and an absorption index of 0.01.

2.4.1.3. Cryogenic transmission electron microscopy. The morphology and size of the colloidal structures present in the emulsions' subnatant phase (section 2.3) were measured by cryogenic transmission electron microscopy (cryo-TEM). For cryo-TEM sample preparation, TEM grids with a graphene oxide (GOx) support layer were used during plunge vitrification. This enabled the preparation of mechanically stable TEM samples with a reduced vitrified water layer thickness which minimizes effects of the embedding medium during imaging and enhances the achievable contrast and resolution for nanometer sized structures [48]. First, the TEM grids were glow-discharged to make the surface of the carbon TEM support film hydrophilic, and 20 μL of GOx aqueous dispersion were deposited on the top of the TEM grid and dried out. Samples for cryo-TEM were then prepared by applying 3 μL of the emulsion subnatant or of Tween 20 aqueous solution (0.5 wt%) on the 200 mesh Cu grid with a R2/2 Quantifoil® carbon support film (Quantifoil MicroTools GmbH) covered with graphene oxide (GOx). An automated vitrification robot (Thermo Fisher Scientific Vitrobot™ Mark IV) was used to blot and plunge the samples into liquid ethane. Cryo-TEM imaging was conducted on the TU/e CryoTitan (Thermo Fisher Scientific), which was operated at 300 kV and is equipped with a Field-Emission Gun, a post column Gatan Energy Filter (GIF, model 2002) and a post-GIF 2k×2k Gatan CCD camera (model 794). Cryo-TEM images were acquired at an electron dose rate of 10 e^{-} $Å^{-2}$ s^{-1} with an exposure time of 2 s at a nominal magnification of 24,000×. An in-house Matlab script was used for measuring the diameter of small droplets from the TEM images (see Figure S1). For the colloid mill-made emulsion, the total number of small oil droplets analyzed for the histogram was 888 (from 14 cryo-TEM images). For the 0.5 wt% and 2.0 wt% emulsion prepared with the Microfluidizer, 316 and 448 droplets (from 12 and 7 cryo-images) were taken for the analysis, respectively.

2.4.2. Oil content determination

The oil content in the subnatant of the centrifuged emulsion samples was quantified using a colorimetric assay for triacylglycerols (Triglycerides Liquicolor Mono kit, HUMAN). In brief, the samples were diluted to a range of 0.4–4 g/L, and about 20 μL of sample were weighed into a 2-mL microtube. Next, 1 mL of assay reagent was added, and the samples were subsequently incubated in a heating block at 800 rpm for 20 min at 20 °C. The absorbance was measured at a wavelength of 500 nm, and the concentration was calculated using a calibration curve (0.4–4 g triglycerides/L).

2.4.3. Lipid extraction

Oil extraction was performed by adding 8 mL hexane–isopropanol (3:1 v/v) to ~ 1.5 mL emulsion and vortexing thoroughly [49]. The mixture was centrifuged at 4,000 × *g* for 20 min and the upper layer, containing the hexane and extracted oil, was carefully separated from the bottom layer. Hexane was evaporated under a stream of nitrogen at 25 °C until constant weight. The remaining oil was stored under inert gas at −80 °C for 48 h to 20 d, before further measurements were performed, which was based on previous research [50].

2.4.4. Lipid oxidation measurement by ^{1}H NMR

Hydroperoxides, aldehydes (primary and secondary oxidation products) and triacylglycerols (reference for total oil amount) were quantified using ^{1}H NMR with an Advance III 600 MHz spectrometer equipped with a 5 mm cryo-probe at 295 K, following the method described by Merkx *et al.* (2018) [51]. In brief, for the whole emulsion samples, 450 μL 5:1 $CDCl_3$/DMSO-d_6 were added to ~ 150 μL extracted oil (as described in 2.4.3) and transferred to 5-mm NMR tubes (Bruker, Billerica, Massachusetts, USA). For the subnatant samples, 580 μL 5:1 $CDCl_3$/DMSO-d_6 were added to ~ 20 μL extracted oil (as described in 2.4.3). From the recorded single pulse experiment, the glycerol backbone peaks at δ 4.4 pm were used for the quantification of the amount of triacylglycerols. From the band selective pulse, the region between δ 13.0 and 8.0 ppm was selectively excited, for the quantification of the lipid oxidation products, following Merkx *et al.* (2018) [51]. The hydroperoxide signals resonate between δ 11.3 and 10.6 ppm and the aldehydes between δ 9.8 and 9.4 ppm. The calculations, including a factor that accounts for intensity loss during the selective pulse, are described in Merkx *et al.* (2018) [51]. The data was processed with Bruker TopSpin 4.0.6 software.

2.5. Estimation of non-adsorbed surfactant concentration

The amount of excess Tween 20 present in the continuous phase was calculated by the following procedure: first the number of droplets (N, in number per kg oil), with a certain droplet radius (r, in m), were calculated:

$$N = \frac{1}{\rho_{oil}} / \frac{4}{3}\pi r^3 \quad (1)$$

where ρ_{oil} is the density of rapeseed oil (920 kg/m^3). The amount of adsorbed surfactant (S_{ad}, in g per kg oil) follows from:

$$S_{ad} = \frac{N\,4\,\pi\,r^2\Gamma}{1000} \quad (2)$$

where Γ (in mg/m^2) is the theoretical mass of adsorbed surfactant per unit of oil–water interface. Since different values for Γ are reported in literature, two different values for Γ were used: 1.5 mg/m^2 [52], and 2.3 mg/m^2 [53]. Finally, the excess concentration of Tween 20 in the continuous phase (C_{excess}, g/L) can be calculated by:

$$C_{excess} = C_{added} - S_{ad} * R_{oil} * \rho_{cont} \quad (3)$$

where C_{added} is the concentration of surfactant in the continuous phase (in g/L), R_{oil} the mass ratio of oil to continuous phase (10 / 90 = 0.111) and ρ_{cont} the density of the continuous (aqueous) phase (which is assumed to be 1.0 kg/L here). The amount of adsorbed surfactant was calculated for both the DLS and SLS results (section 2.4.1), and for each size class, which was weighed by the volume-based presence of that size class. The surface loads obtained from the DLS and SLS results were summed up after weighing them based on the oil content of the subnatant sample (section 2.4.2); we assume that the oil content of the whole emulsion (SLS result) was one minus that of the subnatant. The average of two measurements (DLS, SLS and oil content) was used for calculating the surface area, using two independently prepared emulsions per condition.

2.6. Experimental design

For each measurement, at least two emulsions were prepared independently. Additionally, per data point, two independently incubated samples from the same emulsion were analyzed for the measurements as described in section 2.4. Statistical analysis of variance (F-test and T-

test) (Microsoft Office Excel 2016) was carried out on experimental lipid oxidation values between different samples. Differences at $p < 0.05$ were considered significant.

3. Results and discussion

3.1. Characterization of Tween 20-stabilized emulsions

The droplet size (diameter) distributions (SLS) of 0.5 wt% Tween 20-based emulsion prepared with a lab-scale colloid mill and that of 0.5 or 2.0 wt% Tween 20-based emulsions prepared with a high-pressure homogenizer (Microfluidizer) are shown in Fig. 2a. As expected, the Microfluidizer produced smaller droplets compared to the colloid mill because of the larger shear rates involved [7,54,55]. For the emulsions prepared with the Microfluidizer, the 2.0 wt% Tween 20-based emulsion had a slightly smaller average droplet size than the 0.5 wt% Tween 20-based emulsion. This can be explained by a faster stabilization of small droplets upon homogenization when adding a larger amount of surfactant, therewith preventing immediate re-coalescence of newly made droplets.

When measuring the droplet size distributions of these whole emulsions by static light scattering (SLS), the diameters of the smallest droplets that could be detected (i.e., at the onset of the peak) were ~100 nm for the Microfluidizer-made emulsions and ~300 nm for the colloid mill-made emulsion (Fig. 2a). After centrifugation (28,000 × *g*, 30 min) to remove the largest droplets (creamed phase), smaller colloidal structures in the range of 10–200 nm were detected in the subnatant when analyzed by dynamic light scattering (DLS) (Fig. 2b). These small colloidal structures are most likely a heterogenous population consisting of a mixture of 'swollen micelles' and 'nanoemulsion' droplets, following the terminology defined in section 1.

The droplet size distribution of these 'very small' droplets in the 0.5 wt% Tween 20-based emulsion made with the colloid mill was bimodal, with a high peak around 20 nm and a lower peak around 80 nm. Surprisingly, from the DLS results, the average diameter of structures present in the subnatant of the 0.5 wt% Tween 20-based emulsion made with the colloid mill seemed to be smaller than the 0.5 wt% and 2.0 wt% Tween 20-based emulsions made with the Microfluidizer. The intensity of light scattered (I_{scat}) by colloidal particles scales as $I_{scat} \sim d^6$, with d the droplet diameter. Moreover, in DLS, the z-averaged size is measured: the d_{65} is highly sensitive to the largest colloids present [56]. At this stage, it is important to recall that DLS is known to be an inappropriate method for the analysis of polydisperse emulsions, since it is highly sensitive to: larger colloids/particles, at the expense of smaller co-existing ones [10,45]; contaminant particles [57]; and issues regarding matching the optical settings with the scattering by the droplets [10,58].

Cryo-TEM was employed as an alternative strategy to measure the droplet size distributions in the subnatants. Oil droplets appear as dark round objects with diameters of ~10–100 nm in the cryo-TEM images of subnatants obtained from a colloid mill-made emulsion (Fig. 3a) or from a Microfluidizer-made one (Fig. 3b-3c). The size distributions obtained from image analysis of the cryo-TEM images are shown in Fig. 4 and compared with the number-weighted results from DLS (shown as superimposed solid curves). The cryo-TEM results proved the presence of very small structures with diameters of 10–30 nm (which most likely correspond to swollen micelles) in the subnatants of Tween 20-based emulsions prepared with the Microfluidizer (for both Tween 20 concentrations) (Fig. 4b & 4c), which were not detected by DLS. This highlights the importance of cryo-TEM to assess the presence and size of the tiniest oil-containing structures within polydisperse samples, which may be missed by DLS.

The cryo-TEM results confirmed that the diameters of the very small droplets present in the subnatant of a 0.5 wt% Tween 20-based emulsion made with the colloid mill were, on average, smaller (the major part was 10–30 nm in diameter) compared to those present in the subnatant of the 0.5 wt% Tween 20-based emulsion prepared with the Microfluidizer (Fig. 4a & 4b, respectively). The 0.5 wt% Tween 20-based emulsion made with the colloid mill was calculated to have 0.29–0.36 wt% excess Tween 20 in the continuous phase (depending on the theoretical surface load, section 2.5), whereas this was only 0.0–0.1 wt% for the 0.5 wt% Tween 20-based emulsion made with the Microfluidizer (Table 1). This difference in concentration of Tween 20 in the continuous phase may facilitate the formation of swollen micelles. Another possibility is that due to the larger shear forces exerted in the Microfluidizer, simply more oil becomes dispersed in small droplets, although these droplets have to be quickly stabilized to prevent that they quickly coalesce during homogenization. The droplet size distributions of the 0.5 and 2.0 wt% Tween 20-based Microfluidizer emulsions were very similar (Fig. 4b & 4c), which suggests that within the tested concentration range, the surfactant concentration had almost no influence on the size of the generated very small droplets. With cryo-TEM, very small droplets were

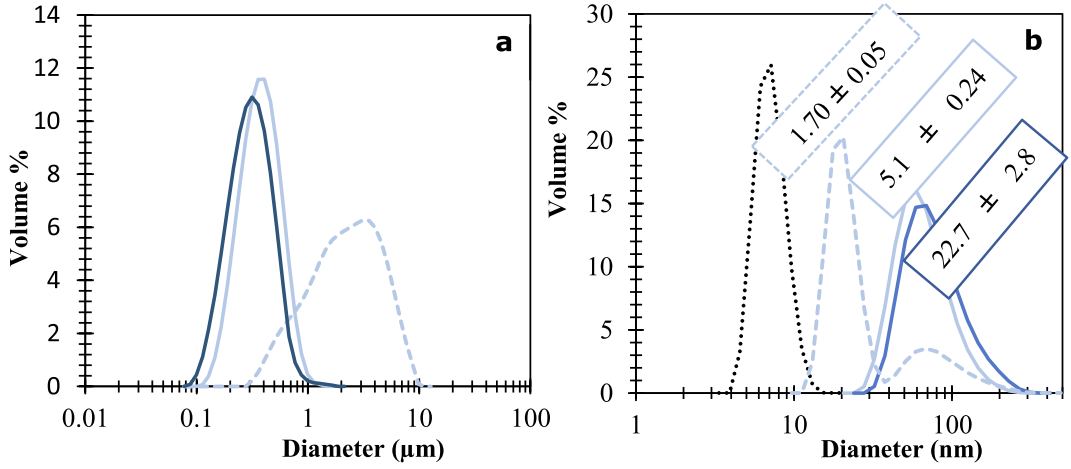

Fig. 2. The droplet size distributions of: (**a**) whole emulsion samples measured by SLS and (**b**) subnatants of centrifuged emulsion samples measured by DLS. Different curves represent different emulsion samples: 0.5 wt% Tween 20 solution as a control (dashed curve, black, only for (**b**)), 0.5 wt% Tween 20-based Microfluidizer emulsion (solid curve, light blue), 2.0 wt% Tween 20-based Microfluidizer emulsion (solid curve, dark blue), and 0.5 wt% Tween 20-based colloid mill emulsion (dashed line, light blue)). The numbers in (**b**) indicate the triglyceride content of the subnatant samples in g/L (whole emulsion contained 100 g/L TAGs). The curves and numbers represent averages of two independently prepared samples that were both measured twice. (For interpretation of the references to colour in this figure legend, the reader is referred to the web version of this article.)

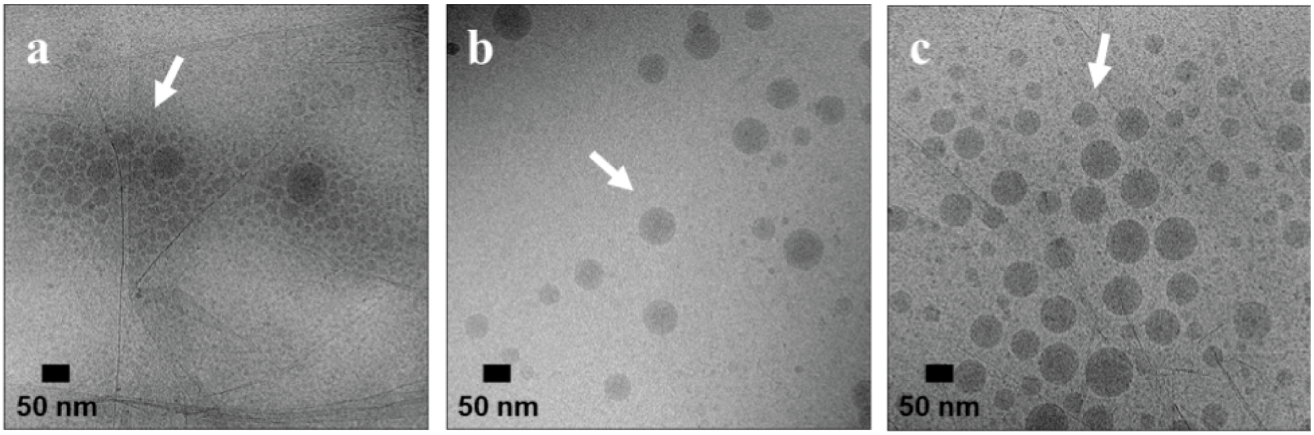

Fig. 3. Representative cryo-TEM images of emulsion subnatants from (**a**) 0.5 wt% Tween 20-based colloid mill emulsion, (**b**) 0.5 wt% Tween 20-based Microfluidizer emulsion, and **(c)** 2.0 wt% Tween 20-based Microfluidizer emulsion at 24000× magnification. Applied nominal defocus value was -1.5 μm. Corresponding cryo-TEM images at 6500× magnification can be found in Supplementary data in Figure S2. White arrows point to oil droplets. Contrast and brightness were adjusted to tune the visibility.

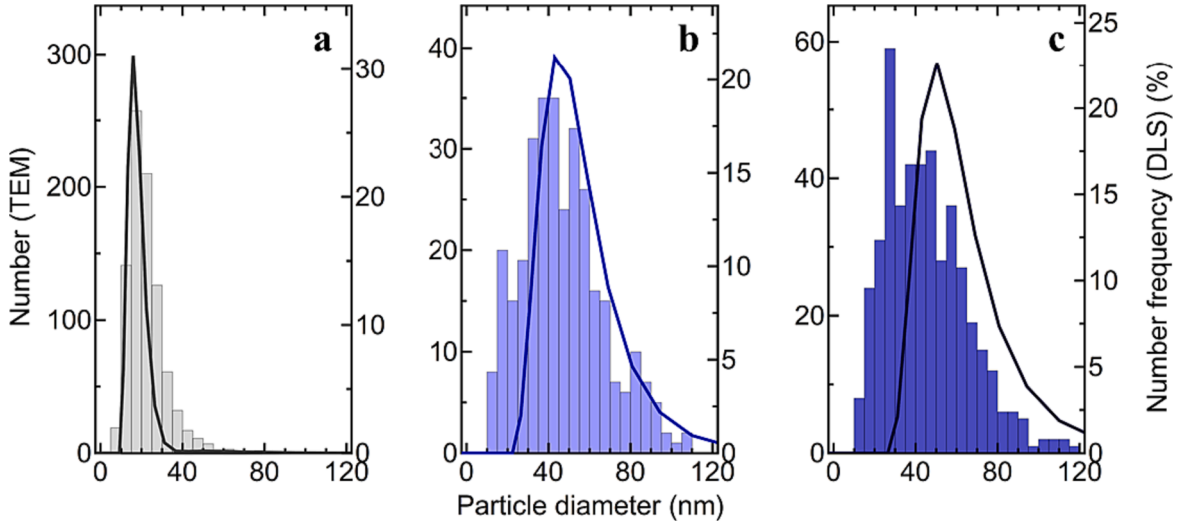

Fig. 4. Diameter distributions of oil droplets obtained from cryo-TEM and DLS (number-weighted hydrodynamic diameter) in subnatants from (**a**) 0.5 wt% Tween 20-based colloid mill emulsion, (**b**) 0.5 wt% Tween 20-based Microfluidizer emulsion and (**c**) 2.0 wt% Tween 20-based Microfluidizer emulsion. Histograms correspond to the size distributions from cryo-TEM data and solid curves correspond to DLS data.

Table 1
Estimated concentrations of excess Tween 20 in the aqueous phase of emulsions. The calculations were performed using theoretical surface loads (Γ) of 1.5 and 2.3 mg/m^2 [52,53].

Emulsification device	Total Tween 20 concentration applied in the aqueous phase (wt. %) (C_{added}, eq. (3))	Theoretical Tween 20 adsorbed (expressed in equivalent wt.% of continuous phase) ($S_{ad} \times R_{oil} \times \rho_{cont}$, eq. (3))	Theoretical excess Tween 20 in continuous phase (wt.%) (C_{excess}, eq. (3))
Colloid mill	0.5	0.14 – 0.21	0.36 – 0.29
Microfluidizer	0.5	0.40 – 0.61*	0.10 – 0*
Microfluidizer	2.0	0.66 – 1.0	1.34 – 0.99

* The calculated value of 0.61 wt% exceeds the total amount used, indicating that there would be no excess at all. This suggests that the high-boundary theoretical surface load of 2.3 mg/m^2 is too high for the present system, in which lower values (closer to the low-boundary value of 1.5 mg/m^2) most likely apply.

observed more frequently throughout all imaged samples when the Tween 20 concentration was increased from 0.5 wt% to 2.0 wt% (Fig. 3). This suggests that more oil becomes dispersed in the very small droplets when more surfactant is present, which was further investigated by measuring the actual oil content of the subnatants. The oil content ranged from 1.7% (±0.05%) of the total oil fraction in the 0.5 wt% Tween 20-based emulsion made with the colloid mill, to 5.1% (±0.24%) in the 0.5 wt% Tween 20-based emulsion made with the Microfluidizer, and even 22.7% (±2.8%) in the 2 wt% Tween 20-based emulsions made with the Microfluidizer (Fig. 2b). Therefore, a 4-fold increase in the surfactant concentration lead to an important shift in the oil partitioning towards the fraction of 'very small droplets' (numbers in Fig. 2b). In contrast, it seems to only moderately change the droplet size distribution of the whole emulsion and of the subnatant (Fig. 2a & b, comparison of both curves).

As mentioned earlier, surfactant micelles in the aqueous phase of emulsions may have two opposing effects in the oxidative stability of emulsions, either due to their ability to exchange reactive molecules between emulsion droplets [16–19,59,60], or due to their protective effect against lipid oxidation [4,53]. Noticeably, micelles could not be

detected in the emulsions' subnatants by DLS (Fig. 2b), even though the theoretical amount of surfactant present in the aqueous phase is much higher than the critical micelle concentration of Tween 20 (0.006 wt% at 25 °C [61]) (Table 1). This can only be explained by the concomitant presence of much larger droplets (>100 nm) that dominate the scattering signal in DLS, as compared to the contribution of the micelles (~8–10 nm) [10,62] (Figs. 1, 2b). To track the potential presence of surfactant micelles in our emulsions, cryo-TEM was used once again. Fig. 5a and 5b show cryo-TEM images of a Tween 20 (0.5.

wt.%) aqueous solution, without any oil added, in which densely packed particles with a diameter of 3–4 nm were observed (indicated with blue arrows in Fig. 5b). This is smaller than the size of Tween 20 micelles of ~8 nm (Fig. 2b) [58,63]. Further analysis of the images by fast Fourier transform (FFT) of the zoomed-in regions revealed that there was a periodic pattern with a spacing of about 0.12 nm^{-1} present, which corresponds to a packing distance of ~8.3 nm (Fig. 5c). This suggests that the hydrophobic cores of Tween 20 micelles can only be seen as darker dots of around 3–4 nm in diameter in the cryo-TEM images, and that the average spacing of 8 nm matches the distance between densely packed Tween 20 micelles. Similar features were observed in the emulsion subnatant from a colloid mill-made emulsion (Fig. 5d–5f), which was in line with our expectations due to an excess of Tween 20 being present in the continuous phase (Table 1). Awad *et al.* [10] also reported the co-existence of micelles and swollen micelles (12–22 nm in diameter) in emulsion systems, which is in line with our findings. In literature, the optically transparent subnatants of such emulsions are sometimes referred to as the continuous phase. For example, a certain amount of hydroperoxides was measured in such a subnatant (centrifugation conditions: 35 min 24,000 × *g*), which may lead to various interpretations depending on the type of colloidal structures actually present [64]. In that case, measurements on the size and amount of physical structures in those subnatants was not performed, so the presence of small droplets with a diameter <200 nm may have been overlooked.

3.2. *Physical and oxidative stability of the co-existing very small emulsion droplets*

Although surfactant micelles have been suggested to play a major role in the oxidative stability of emulsions through exchange of reactive

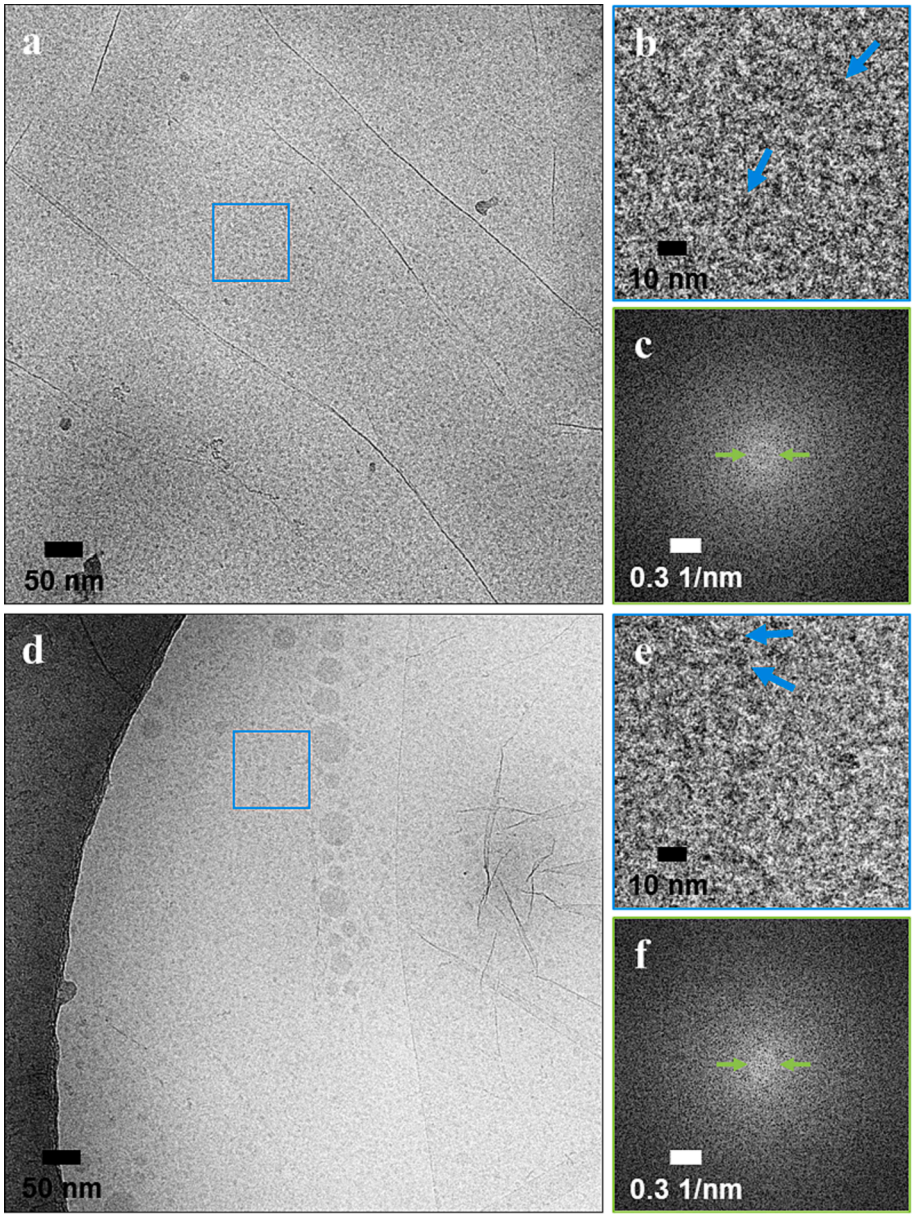

Fig. 5. Representative cryo-TEM images of **(a)** 0.5 wt % Tween 20 aqueous solution and **(d)** 0.5 wt% Tween 20 emulsion subnatant prepared by a colloid mill at 24000× magnification. Applied nominal defocus was -2.5 μm. **(b, e)** Zoomed-in (blue square) regions of (a) and (d). The blue arrows point out to areas where micelle cores clearly appear in black. **(c, f)** Fast Fourier transform of (b) and (e). The green arrows indicate a ring which corresponds to the periodic structure of ~8 nm. Contrast and brightness were adjusted for better visibility. (For interpretation of the references to colour in this figure legend, the reader is referred to the web version of this article.)

molecules between oil droplets [16–19,59,60], or due to their protective effect against lipid oxidation [4,53], here we are mainly interested in the effect of very small droplets. Upon incubation of the colloid mill-made emulsions at 25 °C, the overall droplet size distribution remained constant over the maximum incubation period tested (17 days, Figure S3). Similarly, no major shifts in the droplet size distribution of the smallest detectable droplets occurred over incubation (Fig. 6a). However, based on this DLS data, we cannot exclude that minor shifts might have taken place. In line with this result, no major shifts were observed in the oil content of the subnatant samples containing the very small droplets (Fig. 6b), yet the values at $t_{13}/t_{15}/t_{17}$ were significantly lower than the value at t_0 ($p < 0.05$) (Fig. 6b). This very slight decrease could be due to instabilities such as Ostwald ripening and/or coalescence. Ostwald ripening was not expected to play a major role here because the stripped rapeseed oil used as the oil phase consists mostly of triglycerides, which are virtually insoluble in water [65], but due to the very high Laplace pressure on the very small droplets in combination with the presence of surfactant micelles, it may have occurred slightly. Similarly, coalescence was not expected to play a major role for the very small droplets because the whole emulsion was stable over incubation (Figure S3), but marginal coalescence events may have occurred.

Lipid oxidation products formed in a more prominent way in the very small droplet fraction (◊ in Fig. 7) than in the whole emulsion (□, in Fig. 7), as shown for hydroperoxides (Fig. 7a), and aldehydes (Fig. 7b). For some of the data points, the initial amount ($t = 0$) of lipid oxidation products in the very small droplets was already higher than in the corresponding whole emulsion. The increased formation of lipid oxidation products over time could be due to the large surface area surrounding these very small droplets, which can promote reactions between aqueous pro-oxidants (such as metal ions) and polyunsaturated lipids present in the droplets (Reactions 1–3) [53]. This leads to higher concentrations of radicals, which increases the propagation of lipid oxidation (Reactions 5 & 6). To investigate whether traces of metal ions initiate lipid oxidation in these emulsions, emulsions containing either 75 mg EDTA/kg continuous phase or no EDTA were incubated under the same conditions. EDTA is known to chelate metal ions, which decreases their pro-oxidant effect [66,67]. We found a major decrease in lipid oxidation when adding EDTA to the emulsion (Figure S5), in agreement with previous studies [68–70]. Therefore, in our emulsions (as well as in many model and/or food systems), metal ions play a prominent role in lipid oxidation. These trace amounts of metal ions may originate from the emulsification equipment, from the glassware, or from the ingredients (e.g., Tween 20). Since the smallest droplets have the largest surface-to-volume ratio, the catalysed initiation reactions at the interface (Reactions 1–3) are expected to be most pronounced in the smallest droplets. In addition, initially higher levels of lipid oxidation products are known to increase subsequent lipid oxidation during storage [18,71,72].

Investigations on the effect of droplet size on lipid oxidation, where the differently sized droplets originated from the same emulsions, have been reported previously [25,33]. A recent publication studied the effect of droplet size on lipid oxidation by monitoring the oxidation of the fluorescent dye BODIPY 665/676 in a surfactant-stabilized emulsion, and faster oxidation was found for the smallest droplets (size) compared to the larger droplets (size) [25]. Conversely, in another recent study on mayonnaise, using the same dye, the droplet size did not (or barely) influence the lipid oxidation rate. This was ascribed to the small size difference (1–4 μm) and the possible transfer of the fluorescent dye and/or oxidation products for long incubation periods [33]. Only when stripped oil without antioxidants was used, and thus lipid oxidation proceeded quite rapidly, smaller droplets were found to oxidize slightly faster than larger ones [33]. This highlights that the effect of droplet size on lipid oxidation is often small, if observed at all. In our case, the faster oxidation in small droplets could be highlighted more clearly because the large difference in average size of ± a factor 70 (D[3,2]-based comparison). It should also be pointed out that these two previous studies were based on fluorescent optical microscopy, which does not allow for detection, and thus consideration of the implication of very small droplets (10–200 nm), whereas especially these seem to have a dramatic effect when droplet size is concerned.

When increasing surfactant concentration, more very small droplets are formed (numbers in Fig. 2), which is expected to increase lipid oxidation because of the larger total surface area in the emulsion (Fig. 7). In line with this hypothesis, it was found previously that lipid

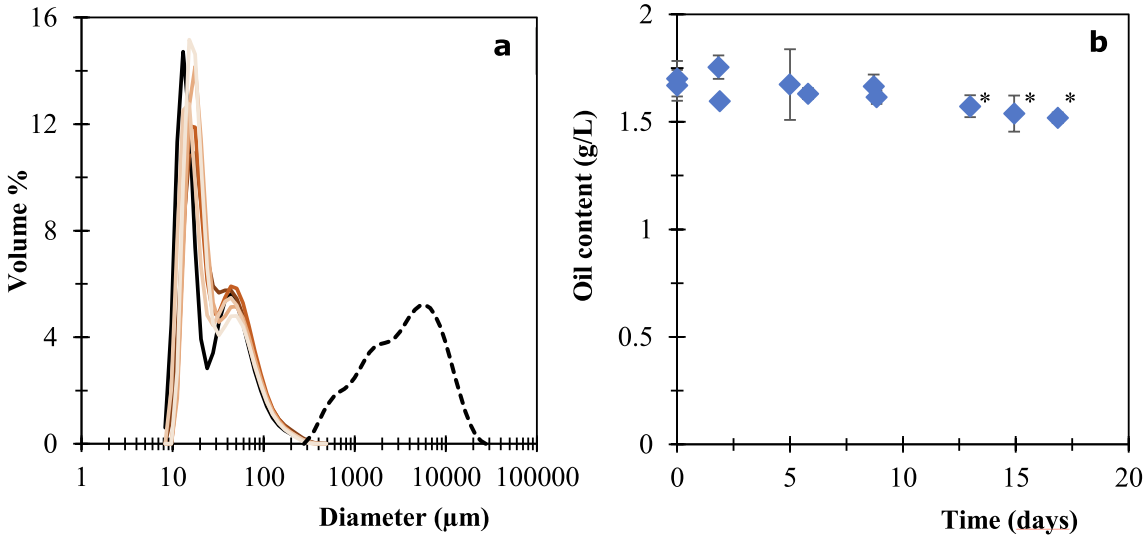

Fig. 6. (**a**) Droplet size distribution in colloid mill-made emulsion samples. The different curves represent the droplet size distributions of the subnatants collected over incubation of an emulsion (by DLS) (solid lines), or of a whole emulsion sample (by SLS) (dashed line); the lighter the colour, the later the timepoint (from t_0 [black] to t_2, t_5, t_7, t_9, and finally t_{15} [light orange]). To allow for checking the graph into more detail, a wider figure containing the same data is shown in Fig. S4a. The curves represent averages of two subnatant samples of one independent replicate; for clarity, the outcome of the other independent replicate is shown in a separate graph in Fig. S4b. (**b**) Oil content in these subnatant samples over incubation, where the * indicates a significant difference between that data point and t_0. The outcomes of the independent replicates are shown as separate data points, and the error bars denote standard deviations of two measurements on two dependent samples (total of 4 measurements per data point). (For interpretation of the references to colour in this figure legend, the reader is referred to the web version of this article.)

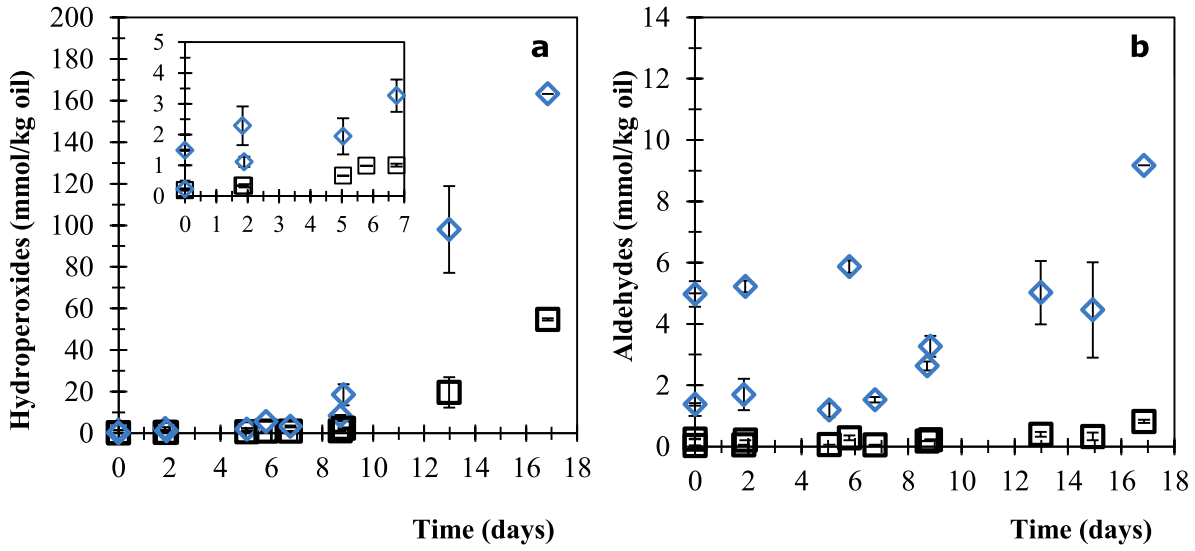

Fig. 7. Formation of hydroperoxides (**a**) and aldehydes (**b**) over incubation of a Tween 20-stabilized emulsions (0.5 wt% Tween 20, colloid mill). Symbols correspond to a different droplet size from the same emulsion: whole emulsion (□) and very small droplets present in the subnatant phase (◇). For the droplet size distributions of the whole emulsion and very small droplets, see Fig. 2a. Error bars denote standard deviations of two measurements on one emulsion sample, and the outcome of independent replicates are shown as separate data points.

oxidation increased with surfactant concentration [73,74]. In contrast, it is known that excess surfactant in the continuous phase may counteract lipid oxidation, which was shown previously by purposely adding excess surfactant post-emulsification [53]. The balance between both effects is probably dependent on the applied conditions and concentrations used, which might explain why in some cases the amount of Tween 20 did not have an effect [75], whereas in other studies lipid oxidation increased with the Tween 20 concentration [73,74]. This, once more, highlights the importance of considering and tracking the very small droplets that can be present in emulsions.

4. Conclusions

In this manuscript, we investigated the occurrence and effect of very small oil droplets and swollen micelles (10–200 nm) in surfactant-stabilized emulsions, which so far have often been overlooked or improperly characterized [10]. Cryo-TEM was shown to be an effective tool to quantify the size of co-existing very small droplets (swollen micelles) and to detect empty surfactant micelles (~8 nm). These smallest structures could not be detected using DLS, most likely due to the dominance of the scattering signal by the larger droplets present.

Increasing the surfactant concentration four times (from 0.5 to 2.0 wt %) led to an increase from 5.1 (±0.24) to 23 (±2.8) wt.% of the total oil becoming incorporated in the very small droplets (10–200 nm). Increasing the mechanical force used to make the emulsion (from colloid mill- to high pressure homogenization) also increased the amount of oil in the very small droplets from 1.7 (±0.05) to 5.1 (±0.24) wt.% of the total oil. Larger shear forces promote droplet elongation during homogenization, which enhances the formation of small droplets, and the increased surfactant concentration quickly stabilizes the newly formed droplets, thereby preventing coalescence during homogenization.

The amount of oil retained in the very small droplets decreased only very slightly over the entire incubation time of the emulsions (17 days). However, the lipid oxidation products were – at any time point – over-represented in the very small droplets. We hypothesize that this is mainly related to their large surface-to-volume ratio compared to the larger droplets present, which favors the contact between traces of pro-oxidants (e.g. metal ions) present in the continuous phase and the unsaturated fatty acids. The forthcoming initiation reactions would promote radical formation, which, in turn, leads to increased propagation of lipid oxidation reactions. The obtained insights are pivotal to improve our understanding of the structural and oxidative characteristics of such emulsion systems.

CRediT authorship contribution statement

Sten ten Klooster: Conceptualization, Data curation, Formal analysis, Investigation, Methodology, Visualization, Writing – original draft. **Machi Takeuchi:** Conceptualization, Data curation, Formal analysis, Investigation, Methodology, Visualization, Writing – original draft. **Karin Schroën:** Conceptualization, Investigation, Methodology, Writing – review & editing, Supervision. **Remco Tuinier:** Conceptualization, Investigation, Methodology, Writing – review & editing, Supervision. **Rick Joosten:** Data curation, Investigation, Methodology. **Heiner Friedrich:** Conceptualization, Investigation, Methodology, Writing – review & editing, Supervision. **Claire Berton-Carabin:** Conceptualization, Investigation, Methodology, Writing – review & editing, Supervision, Funding acquisition.

Declaration of Competing Interest

The authors declare that they have no known competing financial interests or personal relationships that could have appeared to influence the work reported in this paper.

Data availability

Data will be made available on request.

Acknowledgments

This research was funded by the Dutch Research Council (NWO), grant number 731.017.301. We thank the LICENSE project partners and especially Prof. Dr. John van Duynhoven (Unilever and Wageningen University) for useful discussions.

Appendix A. Supplementary data

Supplementary data to this article can be found online at https://doi.org/10.1016/j.jcis.2023.09.005.

References

[1] T.F. Tadros, Emulsion formation, stability, and rheology, in: T.F. Tadros (Ed.), Emuls. Form, Stab., John Wiley & Sons Ltd, 2013, pp. 1–75, https://doi.org/10.1002/9783527647941.ch1.

[2] P. Walstra, Introduction, in: P. Walstra (Ed.), Phys. Chem. Foods, 1st ed., CRC press, 2001 1 8.

[3] D.J. McClements, E.A. Decker, Lipid oxidation in oil-in-water emulsions: Impact of molecular environment on chemical reactions in heterogeneous food systems, J. Food Sci. 65 (2000) 1270–1282, https://doi.org/10.1111/j.1365-2621.2000.tb10596.x.

[4] C.C. Berton-Carabin, M.H. Ropers, C. Genot, Lipid oxidation in oil-in-water emulsions: Involvement of the interfacial layer, Compr. Rev. Food Sci. Food Saf. 13 (2014) 945–977, https://doi.org/10.1111/1541-4337.12097.

[5] K.M. Schaich, Lipid oxidation: theoretical aspects, Bailey's Ind, Oil Fat Prod, 2005.

[6] B. Chen, D.J. McClements, E.A. Decker, Design of foods with bioactive lipids for improved health, Annu. Rev. Food Sci. Technol. 4 (2013) 35–56.

[7] D.J. McClements, Food emulsions: Principles, practices, and techniques, CRC Press, 2004.

[8] F. Leal-Calderon, V. Schmitt, J. Bibette, Emulsion science: Basic principles, Springer Science & Business Media, 2007.

[9] C.C. Berton-Carabin, L. Sagis, K. Schroën, Formation, structure, and functionality of interfacial layers in food emulsions, Annu. Rev. Food Sci. Technol. 9 (2018) 551–587, https://doi.org/10.1146/annurev-food-030117-012405.

[10] T.S. Awad, D. Asker, L.S. Romsted, Evidence of coexisting microemulsion droplets in oil-in-water emulsions revealed by 2D DOSY 1H NMR, J. Colloid Interface Sci. 514 (2018) 83–92.

[11] D.J. McClements, Nanoemulsions versus microemulsions: Terminology, differences, and similarities, Soft Matter 8 (2012) 1719–1729.

[12] B. Vincent, Emulsions, in: T. Cosgrove (Ed.), Colloid Sci. - Princ. Methods Appl, 2nd ed.,, John Wiley & Sons, 2010, pp. 117–133.

[13] S.N. Kale, S.L. Deore, Emulsion micro emulsion and nano emulsion: a review, Syst. Rev. Pharm. 8 (2017) 39.

[14] T. Waraho, D.J. McClements, E.A. Decker, Mechanisms of lipid oxidation in food dispersions, Trends Food Sci. Technol. 22 (2011) 3–13.

[15] B. Chen, D.J. McClements, E.A. Decker, Minor components in food oils: A critical review of their roles on lipid oxidation chemistry in bulk oils and emulsions, Crit. Rev. Food Sci. Nutr. 51 (2011) 901–916.

[16] P. Villeneuve, C. Bourlieu-Lacanal, E. Durand, J. Lecomte, D.J. McClements, E. A. Decker, Lipid oxidation in emulsions and bulk oils: A review of the importance of micelles, Crit. Rev. Food Sci. Nutr. 1–41 (2021).

[17] M. Laguerre, A. Bily, M. Roller, S. Birtić, Mass transport phenomena in lipid oxidation and antioxidation, Annu. Rev. Food Sci. Technol. 8 (2017) 391–411, https://doi.org/10.1146/annurev-food-030216-025812.

[18] M. Laguerre, M. Tenon, A. Bily, S. Birtić, Toward a spatiotemporal model of oxidation in lipid dispersions: A hypothesis-driven review, Eur. J. Lipid Sci. Technol. 122 (2020) 1900209.

[19] P. Villeneuve, E. Durand, E.A. Decker, The need for a new step in the study of lipid oxidation in heterophasic systems, J. Agric. Food Chem. 66 (2018) 8433–8434, https://doi.org/10.1021/acs.jafc.8b03603.

[20] S. ten Klooster, K. Schroën, C. Berton-Carabin, Lipid oxidation products in model food emulsions: Do they stay in or leave droplets, that's the question, Food Chem. 134992 (2022).

[21] K.M. Schaich, Lipid Oxidation: New Perspectives on an Old Reaction, in: Bailey's Ind. Oil Fat Prod., 2020 1 72 10.1002/047167849X.bio067.pub2.

[22] F. Shahidi, Y. Zhong, Lipid oxidation and improving the oxidative stability, Chem. Soc. Rev. 39 (2010) 4067–4079.

[23] J.M.C. Gutteridge, R. Richmond, B. Halliwell, Inhibition of the iron-catalysed formation of hydroxyl radicals from superoxide and of lipid peroxidation by desferrioxamine, The Biochemist. J. 184 (1979) 469–472.

[24] C.P. Dimakou, S.N. Kiokias, I.V. Tsaprouni, V. Oreopoulou, Effect of processing and storage parameters on the oxidative deterioration of oil-in-water emulsions, FoodBiophys. 2 (2007) 38–45.

[25] P. Li, D.J. McClements, E.A. Decker, Application of flow cytometry as novel technology in studying the effect of droplet size on lipid oxidation in oil-in-water emulsions, J. Agric. Food Chem. 68 (2019) 567–573.

[26] S. Gohtani, M. Sirendi, N. Yamamoto, K. Kajikawa, Y. Yamano, Effect of droplet size on oxidation of docosahexaenoic acid in emulsion system, J. Dispers. Sci. Technol. 20 (1999) 1319–1325.

[27] C. Jacobsen, K. Hartvigsen, P. Lund, M.K. Thomsen, L.H. Skibsted, J. Adler-Nissen, G. Hølmer, A.S. Meyer, Oxidation in fish oil-enriched mayonnaise3. Assessment of the influence of the emulsion structure on oxidation by discriminant partial least squares regression analysis, Eur. Food Res. Technol. 211 (2000) 86–98.

[28] L. Lethuaut, F. Métro, C. Genot, Effect of droplet size on lipid oxidation rates of oil-in-water emulsions stabilized by protein, J. Am. Oil Chem. Soc. 79 (2002) 425–430.

[29] V. Rampon, L. Lethuaut, N. Mouhous-Riou, C. Genot, Interface characterization and aging of bovine serum albumin stabilized oil-in-water emulsions as revealed by front-surface fluorescence, J. Agric. Food Chem. 49 (2001) 4046–4051.

[30] K.R. Kuhn, R.L. Cunha, Flaxseed oil–whey protein isolate emulsions: effect of high pressure homogenization, J. Food Eng. 111 (2012) 449–457.

[31] T. Ma, T. Kobayashi, S. Adachi, Effect of droplet size on autoxidation rates of methyl linoleate and α-linolenate in an oil-in-water emulsion, J. Oleo Sci. 62 (2013) 1003–1008.

[32] G. Azuma, N. Kimura, M. Hosokawa, K. Miyashita, Effect of droplet size on the oxidative stability of soybean oil TAG and fish oil TAG in oil-in-water emulsion, J. Oleo Sci. 58 (2009) 329–338.

[33] S. Yang, A.A. Verhoeff, D.W.H. Merkx, J.P.M. van Duynhoven, J. Hohlbein, Quantitative spatiotemporal mapping of lipid and protein oxidation in mayonnaise, Antioxidants. 9 (2020) 1278.

[34] M.A. Neves, Z. Wang, I. Kobayashi, M. Nakajima, Assessment of oxidative stability in fish oil-in-water emulsions: Effect of emulsification process, droplet size and storage temperature, J. Food Process Eng 40 (2017) e12316.

[35] A.F. Horn, N. Barouh, N.S. Nielsen, C.P. Baron, C. Jacobsen, Homogenization pressure and temperature affect protein partitioning and oxidative stability of emulsions, J. Am. Oil Chem. Soc. 90 (2013) 1541–1550.

[36] S.P. O'Dwyer, D. O'Beirne, D.N. Eidhin, B.T. O'Kennedy, Effects of sodium caseinate concentration and storage conditions on the oxidative stability of oil-in-water emulsions, Food Chem. 138 (2013) 1145–1152.

[37] D. Ries, A. Ye, D. Haisman, H. Singh, Antioxidant properties of caseins and whey proteins in model oil-in-water emulsions, Int. Dairy J. 20 (2010) 72–78.

[38] K. Nakaya, H. Ushio, S. Matsukawa, M. Shimizu, T. Ohshima, Effects of droplet size on the oxidative stability of oil-in-water emulsions, Lipids 40 (2005) 501–507.

[39] M.B. Let, C. Jacobsen, A.-D.-M. Sørensen, A.S. Meyer, Homogenization conditions affect the oxidative stability of fish oil enriched milk emulsions: lipid oxidation, J. Agric. Food Chem. 55 (2007) 1773–1780.

[40] L. Atarés, L.J. Marshall, M. Akhtar, B.S. Murray, Structure and oxidative stability of oil in water emulsions as affected by rutin and homogenization procedure, Food Chem. 134 (2012) 1418–1424.

[41] M. Costa, S. Losada-Barreiro, C. Bravo-Díaz, A.A. Vicente, L.S. Monteiro, F. Paiva-Martins, Influence of AO chain length, droplet size and oil to water ratio on the distribution and on the activity of gallates in fish oil-in-water emulsified systems: Emulsion and nanoemulsion comparison, Food Chem. 310 (2020) 125716.

[42] S. Kiokias, C. Dimakou, V. Oreopoulou, Effect of heat treatment and droplet size on the oxidative stability of whey protein emulsions, Food Chem. 105 (2007) 94–100.

[43] H.T. Osborn, C.C. Akoh, Effect of emulsifier type, droplet size, and oil concentration on lipid oxidation in structured lipid-based oil-in-water emulsions, Food Chem. 84 (2004) 451–456.

[44] M. Costa, J. Freiría-Gándara, S. Losada-Barreiro, F. Paiva-Martins, C. Bravo-Díaz, Effects of droplet size on the interfacial concentrations of antioxidants in fish and olive oil-in-water emulsions and nanoemulsions and on their oxidative stability, J. Colloid Interface Sci. 562 (2020) 352–362.

[45] S.M. Patil, D.A. Keire, K. Chen, Comparison of NMR and dynamic light scattering for measuring diffusion coefficients of formulated insulin: implications for particle size distribution measurements in drug products, AAPS J. 19 (2017) 1760–1766.

[46] H. Friedrich, P.M. Frederik, G. De With, N.A.J.M. Sommerdijk, Imaging of self-assembled structures: Interpretation of TEM and Cryo-TEM images, Angew. Chemie - Int. Ed. 49 (2010) 7850–7858, https://doi.org/10.1002/anie.201001493.

[47] C. Berton, C. Genot, M.-H. Ropers, Quantification of unadsorbed protein and surfactant emulsifiers in oil-in-water emulsions, J. Colloid Interface Sci. 354 (2011) 739–748, https://doi.org/10.1016/J.JCIS.2010.11.055.

[48] M.W.P. van de Put, J.P. Patterson, P.H.H. Bomans, N.R. Wilson, H. Friedrich, R.A. T.M. Van Benthem, G. De With, R.K. O'Reilly, N.A.J.M. Sommerdijk, Graphene oxide single sheets as substrates for high resolution cryoTEM, Soft Matter 11 (2015) 1265–1270, https://doi.org/10.1039/c4sm02587c.

[49] T. Waraho, D.J. McClements, E.A. Decker, Impact of free fatty acid concentration and structure on lipid oxidation in oil-in-water emulsions, Food Chem. 129 (2011) 854–859.

[50] S. ten Klooster, P. Villeneuve, C. Bourlieu-Lacanal, E. Durand, K. Schroën, C. Berton-Carabin, Alkyl chain length modulates antioxidant activity of gallic acid esters in spray-dried emulsions, Food Chem. 387 (2022) 132880.

[51] D.W.H. Merkx, G.T.S. Hong, A. Ermacora, J.P.M. Van Duynhoven, Rapid quantitative profiling of lipid oxidation products in a food emulsion by 1H NMR, Anal. Chem. 90 (2018) 4863–4870.

[52] M.A. Bos, T. Van Vliet, Interfacial rheological properties of adsorbed protein layers and surfactants: a review, Adv. Colloid Interface Sci. 91 (2001) 437–471.

[53] C. Berton, M.-H. Ropers, M. Viau, C. Genot, Contribution of the interfacial layer to the protection of emulsified lipids against oxidation, J. Agric. Food Chem. 59 (2011) 5052–5061.

[54] K. Schroën C.C. Berton-Carabin Emulsification: Established and Future Technologies, in: H.G. Merkus, G.M.H. Meesters (Eds.), Prod. Handl. Charact. Part. Mater. Springer International Publishing, 2016 257 289 10.1007/978-3-319-20949-4_8.

[55] P. Walstra, Principles of emulsion formation, Chem. Eng. Sci. 48 (1993) 333–349.

[56] J.K.G. Dhont Chapter 3 Light scattering, in: J.K.G. Dhont (Ed.), Stud. Interface Sci., Elsevier, 1996 107 170 10.1016/S1383-7303(96)80005-6.

[57] H. Ruf, Treatment of contributions of dust to dynamic light scattering data, Langmuir 18 (2002) 3804–3814.

[58] N. Pal, S.D. Verma, M.K. Singh, S. Sen, Fluorescence correlation spectroscopy: an efficient tool for measuring size, size-distribution and polydispersity of microemulsion droplets in solution, Anal. Chem. 83 (2011) 7736–7744.

[59] P. Li, D.J. McClements, E.A. Decker, Application of flow cytometry as novel technology in studying lipid oxidation and mass transport phenomena in oil-in-water emulsions, Food Chem. 315 (2020) 126225.

[60] D.J. McClements, S.R. Dungan, J.B. German, J.E. Kinsella, Oil exchange between oil-in-water emulsion droplets stabilised with a non-ionic surfactant, FoodHydrocoll. 6 (1992) 415–422.

[61] M.E. Mahmood, D.a.F. Al-koofee, Effect of temperature changes on critical micelle concentration for tween series surfactant, Glob. J. Sci. Front. Res. Chem. 13 (2013) 1–7.

[62] S.J. Law, M.M. Britton, Sizing of reverse micelles in microemulsions using NMR measurements of diffusion, Langmuir 28 (2012) 11699–11706.
[63] S. Mandal, C. Banerjee, S. Ghosh, J. Kuchlyan, N. Sarkar, Modulation of the photophysical properties of curcumin in nonionic surfactant (Tween-20) forming micelles and niosomes: A comparative study of different microenvironments, J. Phys. Chem. B 117 (2013) 6957–6968.
[64] C.D. Nuchi, P. Hernandez, D.J. McClements, E.A. Decker, Ability of lipid hydroperoxides to partition into surfactant micelles and alter lipid oxidation rates in emulsions, J. Agric. Food Chem. 50 (2002) 5445–5449.
[65] N.K. Andrikopoulos, Triglyceride species compositions of common edible vegetable oils and methods used for their identification and quantification, Food Rev. Int. 18 (2002) 71–102, https://doi.org/10.1081/FRI-120003418.
[66] J. Lee, E.A. Decker, Effects of metal chelator, sodium azide, and superoxide dismutase on the oxidative stability in riboflavin-photosensitized oil-in-water emulsion systems, J. Agric. Food Chem. 59 (2011) 6271–6276.
[67] I. Bayram, E.A. Decker, Underlying mechanisms of synergistic antioxidant interactions during lipid oxidation, Trends Food Sci, Technol, 2023.
[68] J. Alamed, D.J. McClements, E.A. Decker, Influence of heat processing and calcium ions on the ability of EDTA to inhibit lipid oxidation in oil-in-water emulsions containing omega-3 fatty acids, Food Chem. 95 (2006) 585–590.
[69] J.R. Mancuso, D.J. McClements, E.A. Decker, Iron-accelerated cumene hydroperoxide decomposition in hexadecane and trilaurin emulsions, J. Agric. Food Chem. 48 (2000) 213–219.
[70] L. Mei, E.A. Decker, D.J. McClements, Evidence of iron association with emulsion droplets and its impact on lipid oxidation, J. Agric. Food Chem. 46 (1998) 5072–5077.
[71] K. Schroën, C.C. Berton-Carabin, A unifying approach to lipid oxidation in emulsions: Modelling and experimental validation, Food Res. Int. 111621 (2022).
[72] Y. Yoshida, E. Niki, Oxidation of methyl linoleate in aqueous dispersions induced by copper and iron, Arch. Biochem. Biophys. 295 (1992) 107–114.
[73] M. Kargar, F. Spyropoulos, I.T. Norton, The effect of interfacial microstructure on the lipid oxidation stability of oil-in-water emulsions, J. Colloid Interface Sci. 357 (2011) 527–533.
[74] K.I.S. Rhee, Factors affecting oxygen uptake in model systems used for investigating lipid peroxidation in meat, J. Food Sci. 43 (1978) 6–9.
[75] L. Ponginebbi, W.W. Nawar, P. Chinachoti, Oxidation of linoleic acid in emulsions: Effect of substrate, emulsifier, and sugar concentration, J. Am. Oil Chem. Soc. 76 (1999) 131.